Acceleration of Gradient-Based Algorithms for Array Antenna Synthesis with Far Field or Near Field Constraints

Daniel R. Prado, Álvaro F. Vaquero, Manuel Arrebola, *Senior Member, IEEE,* Marcos R. Pino, and Fernando Las-Heras, *Senior Member, IEEE*

***Abstract*—This work presents a technique for the acceleration of gradient-based algorithms that employ finite differences in the calculation of the gradient for the optimization of array antennas. It is based on differential contributions, which takes advantage of the fact that when an array is optimized, each element is analyzed independently from the rest. Thus, the computation of the gradient of the cost function, which is typically the most time consuming operation of the algorithm, can be accelerated. A time cost study is presented and the technique is implemented, as an example, in the generalized Intersection Approach algorithm for array optimization in near and far fields. Several syntheses are performed to assess the improvement of this technique. In the far field, it is compared for periodic and aperiodic arrays using different approaches for the computation of the gradient, including the analytic derivative. A reflectarray is also optimized in the near field with the goal of improving its quiet zone. The technique of differential contributions shows important reductions in the time per iteration in all three syntheses, specially in that of aperiodic arrays and near field optimization, where the time saved in the evaluation of the gradient is greater than 99%.**

***Index Terms*—Gradient-based algorithm, optimization, synthesis, aperiodic array, reflectarray, near field, far field, differential contributions, finite differences**

I. Introduction

ARRAY synthesis is important for applications that require non-canonical patterns, either in near or far field regions. There are several ways to synthesize the desired pattern, for instance, analytical techniques [1]–[3], although they present limitations when applied to complex shaped patterns. A more powerful approach is to employ some optimization algorithm (given some suitable starting point), which can be divided into two general groups depending on how they navigate the search space: global or local. Global optimization algorithms include some well known algorithms such as genetic algorithms [4] or particle swarm optimization [5], among others. They perform an exhaustive search and, in principle, do not depend on the starting point. However, they take many iterations to converge and, as the search space grows exponentially with the number of optimizing variables, they are only practical for arrays with a moderate number of elements. From a computationally point of view, the main advantage of these algorithms is that the time per iteration is fast and mainly depends on the number of population members which are being considered, and they are commonly fewer than the number of optimizing variables [5], [6].

On the other hand, local search algorithms strongly depend on the starting point and perform a local search in the vicinity of that point, which will lead in general to a local minimum. There are many local search algorithms for array synthesis, such as the steepest descent [7], conjugate gradient [8], intersection approach [9], Levenberg-Marquardt [10] or Broyden-Fletcher-Goldfarb-Shanno [11]. These algorithms require the computation of a gradient to obtain the direction in which the search space is traversed, following the path with maximum gradient in order to minimize a cost function. For this reason, local search algorithms sometimes are referred to as gradient-based algorithms. In addition, the computation of the gradient is usually the most time consuming operation. The only exception is the intersection approach since it is based on a different concept (i.e., the intersection between two sets [9], [12], [13]). Nevertheless, the generalized intersection approach, with improved convergence [13], also employs a gradient-based algorithm in one of its projectors [14], [15]. In addition, local search algorithms are sometimes used along with global search algorithms, obtaining the so-called hybrid algorithms, which perform local searches in certain regions to refine the results provided by the global search [16], [17].

When using gradient-based algorithms, it is best to analytically compute the gradient in order to accelerate computations. This can be done either for near [18] or far fields [19]. However, there are cases in which there is no direct expression relating the optimizing variables and the cost function, for instance when using the Method of Moments [15], look-up tables [20], Artificial Neural Networks (ANN) [21] or Support Vector Machines (SVM) [22]. Also, there might be cases in which the derivatives may be cumbersome to obtain. In such

This work was supported in part by the European Space Agency (ESA) under contract ESTEC/AO/1-7064/12/NL/MH; by the Ministerio de Ciencia, Innovación y Universidades under project TEC2017-86619-R (ARTEINE), and through Programa "Clarín" de Ayudas Postdoctorales / Marie Courie-Cofund under project ACA17-09.

D. R. Prado is with the Institute of Sensors, Signals and Systems, School of Engineering and Physical Sciences, Heriot-Watt University, Edinburgh, U.K. (email: dr38@hw.ac.uk).

A. F. Vaquero, M. Arrebola, M. R. Pino and F. Las-Heras are with the Department of Electrical Engineering, Group of Signal Theory and Communications, Universidad de Oviedo, Gijón, Spain (e-mail: avaquero@tsc.uniovi.es; arrebola@uniovi.es; mpino@uniovi.es; flasheras@uniovi.es).

Color versions of one or more of the figures in this paper are available online at http://ieeexplore.ieee.org.

Digital Object Identifier XX.XXXX/TAP.XXXX.XXXXXXX

cases, the gradient may be computed using finite differences. Another approach is to employ the Adjoint Variable Methods (AVM) [23]–[27], a powerful class of techniques that allows to obtain the sensitivities (derivatives) with regard to any design parameter using at most one extra full-wave simulation of the whole structure. They have been employed with success for the optimization of electromagnetic devices such as filters [24] or antennas [25], [26] by improving their scattering matrix response. However, considering other antenna factors, such as the far field for radiation pattern synthesis, is still an open area of research using AVM [25].

This paper introduces the technique of differential contributions in order to accelerate the computation of the gradient for local search or hybrid algorithms in array synthesis when it is implemented with finite differences. It is based on the fact that in array synthesis each element is analyzed independently from the rest, and also in the linearity of Maxwell's equations, which leads to a linear dependence between the field in the aperture and the radiated field (either near field or far field). Thus, when each derivative is evaluated, only the differential contribution of the considered element is taken into account in the computations, saving computing time. This strategy is implemented in the generalized Intersection Approach and a time cost study is performed both in near and far field. For the far field case, this technique is compared with the analysis of a periodic reflectarray with the Fast Fourier Transform (FFT) and an aperiodic array with the Non-Uniform FFT (NUFFT), along with the analytic derivative of the cost function. For the near field case, a reflectarray is considered with the goal of improving its quiet zone. In all three cases the technique of differential contributions reduces the computing time of evaluating the gradient with finite differences, and it is also faster than the analytic derivative. Remarkable improvements are obtained in the far field for aperiodic arrays and in the near field. Moreover, with this technique, the synthesis of aperiodic arrays, which is slower due to the use of the NUFFT instead of the FFT, is leveled with the synthesis of periodic arrays, since the use of the FFT/NUFFT is avoided in the computation of the gradient.

The paper is organized as follows. Section II introduces the formulation of the technique of differential contributions for the evaluation of the gradient. Section III contains a study of the time cost for computing the gradient with different methods. Section IV shows the results obtained for an implementation of the technique in the generalized Intersection Approach. Section V presents three different array syntheses to show the total time savings with relevant examples. Finally, Section VI has the conclusions.

II. Computation of the Gradient

A. Introduction

Let us suppose an array of N elements whose radiated field (either near or far field) is computed at M points. The goal is to accelerate the computation of the gradient of a cost function to shape the radiated field pattern. For this task we assume that S variables are optimized, which may be $S \leq N$ if we are optimizing only a subset of the array elements, $S > N$ if there are several variables per array element which are optimized (for instance, when directly optimizing the element geometry, as in [15], or for phase-only synthesis if synthesizing two polarizations at the same time), or combinations of the two.

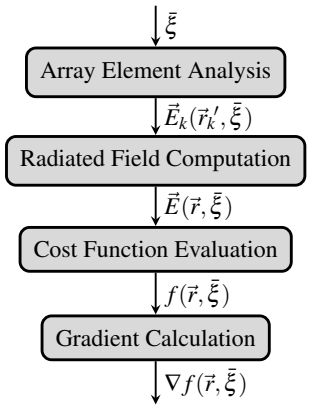

Fig. 1. Flowchart for the computation of the cost function gradient.

The gradient of a multidimensional scalar function is:

$$\nabla f(\vec{r}, \bar{\xi}) = \left(\frac{\partial f(\vec{r}, \bar{\xi})}{\partial \xi_1}, \cdots, \frac{\partial f(\vec{r}, \bar{\xi})}{\partial \xi_i}, \cdots, \frac{\partial f(\vec{r}, \bar{\xi})}{\partial \xi_S} \right), \quad (1)$$

where $\bar{\xi} = (\xi_1, \ldots, \xi_i, \ldots, \xi_S)$ is a vector of S optimizing variables and $\vec{r} \in \{\vec{r}_1, \ldots, \vec{r}_t, \ldots, \vec{r}_M\}$ an observation point where the radiated field is computed. Each iteration of the algorithm estimates the derivatives. The ideal case is to solve the derivatives analytically, since in such case the computation of the gradient in (1) will be faster. Otherwise, each derivative is computed using finite differences, for instance a forward or backward finite difference since they save half the calls to the cost function with regard to the central difference. For instance, the backward lateral difference takes the form:

$$\frac{\partial f(\vec{r}, \bar{\xi})}{\partial \xi_i} = \frac{f(\vec{r}, \bar{\xi}) - f(\vec{r}, \bar{\xi} - h\hat{e}_i)}{h} + \mathcal{O}(h), \quad (2)$$

where h is a small positive scalar which can be optimally selected depending on the type of finite difference (central or lateral) [10], and $\hat{e}_i$ is the ith unit vector such that:

$$\bar{\xi} - h\hat{e}_i = (\xi_1, \ldots, \xi_i - h, \ldots, \xi_S). \quad (3)$$

Once the optimal value of h is selected [10], it remains fixed for the computation of all derivatives.

The process for the computation of the gradient (1) can be divided into the following steps, as illustrated in Fig. 1:

1) Starting with the optimizing variables $\bar{\xi}$, that can be geometrical dimensions in general optimization, or the phase-shift introduced by the array elements in the particular case of Phase-Only Synthesis (POS), the tangential field $\vec{E}_k(\vec{r}_k', \bar{\xi})$ at the array aperture is calculated.
2) The radiated field $\vec{E}(\vec{r}, \bar{\xi})$ is obtained using the tangential field as source.
3) Computation of the cost function $f(\vec{r}, \bar{\xi})$ that will depend on the synthesis algorithm.
4) The derivatives are calculated to obtain the gradient.

The technique of differential contributions requires that two conditions are met. First, the modification of one variable does

not affect other variables. And second, part of the process for the calculation of the cost function is linear.

The first condition is met when the analysis of each array element is independent from the rest, i.e. assuming local periodicity. Despite this condition, the coupling between elements may be taken into account. If a Full-Wave analysis technique based on Local Periodicity (FW-LP) is employed in the optimization, such as in [15], mutual coupling is taken into account directly during the synthesis procedure. On the other hand, the condition is also met in the case of POS, which is very common in array pattern synthesis. In POS, the mutual coupling is considered in a further step during the design process of the array elements or the feeding network to match the phase distribution obtained in the synthesis stage [28].

In order to fulfill the second condition, the entire process for the calculation of the gradient or part of it must be linear. Ideally, this linear relation would be between the optimizing variable ξ_i and the cost function f. In practice, this is not true for array antenna synthesis. Indeed, it is common to employ non-linear cost functions which breaks the linear relation. Looking into each step of the process, the first one concerning the computation of the tangential field starting from the optimizing variables is, in general, non-linear; such is the case in phased-arrays or when carrying out a direct geometry optimization [15], [20]. In addition, the relation between the radiated field and cost function (step 3) is, in general, also non-linear [14], [15], [29]. However, due to the linearity of Maxwell's equations, the relation between the tangential field and the radiated field (either near or far field) is linear (step 2), and this can be exploited in array antenna synthesis to accelerate the computation of the gradient by applying the technique of differential contributions to the computation of the radiated field from the field at the aperture.

B. Differential Contribution for Radiated Field Calculation

Continuing with (2), for the computation of $f(\vec{r},\bar{\xi})$ the radiated field $\vec{E}(\vec{r},\bar{\xi})$ must be obtained. Similarly, for the computation of $f(\vec{r},\bar{\xi}-h\hat{e}_i)$, the field $\vec{E}(\vec{r},\bar{\xi}-h\hat{e}_i)$ is required. Since the modification of one variable does not affect the rest, the perturbed field $\vec{E}(\vec{r},\bar{\xi}-h\hat{e}_i)$ can be computed by extracting the original contribution of the unperturbed array element and adding the contribution of the perturbed element. Using the differential contribution we have:

$$\vec{E}(\vec{r},\bar{\xi}-h\hat{e}_i)=\vec{E}(\vec{r},\bar{\xi})+\Delta\vec{E}(\vec{r},\xi_i), \tag{4}$$

where $\Delta\vec{E}(\vec{r},\xi_i)$ is the differential contribution to the radiated field produced by the array element depending on variable i:

$$\Delta\vec{E}(\vec{r},\xi_i)=\vec{E}(\vec{r},\xi_i-h)-\vec{E}(\vec{r},\xi_i). \tag{5}$$

Since $\vec{E}(\vec{r},\bar{\xi})$ is computed once for all S derivatives in (1), the field in (4) is computed by taking into account the differential contribution of one element only, thus accelerating the computation of the perturbed radiated field, which will reduce the computing time of evaluating (2). Note, however, that there is no linear relation between ξ_i and $\vec{E}(\vec{r},\xi_i)$. Instead, the linear relation is between the tangential field and the radiated field.

Let us call $\vec{E}_k(\vec{r}_k')$ the tangential field of the kth array element at location $\vec{r}_k'$, with $k=1,\ldots,N$. Since the number of optimizing variables S is in general different from the number of array elements N, we will denote by $\vec{E}_k(\vec{r}_k',\xi_i)$ the tangential field of the kth array element which depends on optimizing variable i (i.e. ξ_i), with $i=1,\ldots,S$. When an array element does not depend on an optimizing variable, $\vec{E}_k(\xi_i)=\vec{E}_k$, dropping the $\vec{r}_k'$ to alleviate notation.

Thus, (5) can be expressed writing the radiated field as a function of the tangential field:

$$\Delta\vec{E}(\vec{r},\xi_i)=\vec{E}(\vec{r},\vec{E}_k(\xi_i-h))-\vec{E}(\vec{r},\vec{E}_k(\xi_i)). \tag{6}$$

Since the radiated field is linear with respect to the tangential field, it follows:

$$\Delta\vec{E}(\vec{r},\xi_i)=\vec{E}(\vec{r},\Delta\vec{E}_k(\xi_i)), \tag{7}$$

where:

$$\Delta\vec{E}_k(\xi_i)=\vec{E}_k(\xi_i-h)-\vec{E}_k(\xi_i). \tag{8}$$

This way, instead of evaluating two radiated fields at M points, as in (5) or (6), it is only necessary to calculate the difference between tangential fields in (8) and then to evaluate one radiated field in (7).

The particularization for the far field and near field cases is straightforward and will be addressed in the following section.

C. Differential Contributions for Far Field Analysis

For the far field case, the radiated field can be expressed as:

$$\vec{E}_{\text{FF}}(\vec{r},\bar{\xi})=\sum_{k=1}^{N}e_{p,k}(\vec{r})\,\vec{E}_k(\xi_i)\exp\left(j\,k_0\,\vec{r}\cdot\vec{r}_k'\right), \tag{9}$$

where $\vec{r}\in\{\vec{r}_1,\ldots,\vec{r}_t,\ldots,\vec{r}_M\}$ is a vector of observation points in the far field, with $\vec{r}=(u,v)$ and $u=\sin\theta\cos\varphi$, $v=\sin\theta\sin\varphi$; $\vec{r}_k'$ is the coordinate vector of the kth array element; $e_p(\vec{r})$ is a scalar function representing the element pattern, which in general will be different for each array element, and it also includes the propagation term for compactness; and $\vec{E}_k(\xi_i)$ is the tangential field on the kth array element which may depend on variable ξ_i.

The computation of the modified far field is then:

$$\vec{E}_{\text{FF}}(\vec{r},\bar{\xi}-h\hat{e}_i)=\vec{E}_{\text{FF}}(\vec{r},\bar{\xi})+\vec{E}_{\text{FF}}(\vec{r},\Delta\vec{E}_k(\xi_i)), \tag{10}$$

where the differential contribution to the far field is:

$$\Delta\vec{E}_k(\xi_i)=\vec{E}_k(\xi_i-h)-\vec{E}_k(\xi_i). \tag{11}$$

This is a direct application of (4)–(8) to the far field case, and allows to calculate the derivative in (2) by evaluating the far field only once for just one array element.

D. Differential Contributions for Near Field Analysis

For the near field synthesis, the near field model described in [30] is employed. It is based on computing the near field at any point in the semispace in front of the array as far field contributions of each array element, which are modeled as small rectangular apertures, thus taking into account the

element amplitude pattern. This way, the near field at any point in space may be expressed as:

$$\vec{E}_{\text{NF}}(\vec{r},\bar{\xi}) = \mathcal{T}_2\left\{\sum_{k=1}^{N}\mathcal{T}_1\left\{\vec{E}_{\text{FF},k}(\vec{r},\xi_i)\right\}\right\}, \tag{12}$$

where $\vec{r} \in \{\vec{r}_1,\ldots,\vec{r}_t,\ldots,\vec{r}_M\}$ is the set of observation points in a volume in front of the array, with $\vec{r}=(x,y,z)$; $\vec{E}_{\text{FF},k}(\vec{r},\xi_i)$ is the far field contribution at $\vec{r}$ of the kth array element, whose tangential field is $\vec{E}_k(\xi_i)$; and $\mathcal{T}_1\{\cdot\}$ and $\mathcal{T}_2\{\cdot\}$ perform linear transformations with respect to the tangential field, a change of coordinates from spherical to Cartesian and a rotation, respectively [30]. Please note that depending on the antenna optics, the $\mathcal{T}_2$ operator might be the identity [30].

The same considerations as before can be made for the near field, and since $\mathcal{T}_1$ and $\mathcal{T}_2$ perform a linear transformation, the modified near field can also be computed using the differential contribution as:

$$\vec{E}_{\text{NF}}(\vec{r},\bar{\xi}-h\hat{e}_i) = \vec{E}_{\text{NF}}(\vec{r},\bar{\xi}) + \vec{E}_{\text{NF}}(\vec{r},\Delta\vec{E}_k(\xi_i)), \tag{13}$$

where $\Delta\vec{E}_k(\xi_i)$ is defined in (11).

III. Computational Cost

The analysis of the computational cost of the gradient (1) is divided into two blocks to highlight the improvement of this work. The first block corresponds to the analysis of the array elements depending on their modeling. The second block includes the rest of the steps of Fig. 1, computing the gradient starting from the field at the aperture.

A. Time Cost of Computing the Tangential Field

When performing array synthesis there are several possibilities for the computation of $E_k(\xi_i)$. First, the tangential field $E_k(\xi_i)$ might be the optimizing variable [31], in which both the optimal amplitude and phase are sought. In such case, the time cost of analyzing the element can be assimilated to $\mathcal{O}(1)$.

However, if a direct optimization of the array element geometry is performed employing a FW-LP [32]–[34], obtaining $E_k(\xi_i)$ becomes slower and its time cost is denoted as $\mathcal{O}(O_{\text{FW-LP}})$. An intermediate case would be to model the array element with ANN [21], SVM [22] or use Look-Up Tables (LUT) [20], which considerably accelerates the computation of $E_k(\xi_i)$ with regard to the FW-LP. In any case, we can assume a time cost $\mathcal{O}(O_{\text{Elem}})$ for the element analysis, which will take one form or another depending on the employed analysis method. The time cost of analyzing the element is independent of the improvement provided by the differential contribution technique and should be added to the time cost of the techniques described in Section III-B.

B. Time Cost for the Gradient Computation

Starting from the tangential field at the aperture, a direct evaluation of $f(\vec{r},\bar{\xi})$ has a computational cost of $\mathcal{O}(NM)$. Thus, if S variables are optimized, the computational cost of the gradient is:

$$\mathcal{O}(SNM). \tag{14}$$

However, if the derivative can be obtained as an analytical function, the time cost is reduced to:

$$\mathcal{O}(SM). \tag{15}$$

Equations (14) and (15) can be considered as the upper and lower limits of the time cost of a general technique, both in near and far field problems. Unfortunately, this is a particular case and, in general, numerical evaluation of the derivatives is required, for which several techniques can be applied.

1) Computational Cost in Far Field Analysis of Uniform Arrays: A direct evaluation of the far field is inefficient, since (9) can be efficiently computed with an FFT. If there are not analytic derivatives, and they are evaluated by finite differences, the time cost of evaluating the gradient would be:

$$\mathcal{O}(SM\log M) \tag{16}$$

2) Computational Cost in Far Field Analysis of Non-Uniform Arrays: For aperiodic arrays, the radiation pattern has the same expression as in (9), with the only difference that the array elements are arranged in a non-regular lattice. Now, the NUFFT must be used, which for planar aperiodic arrays yields a time cost for the gradient evaluation [35]:

$$\mathcal{O}\left(SM\left(\log M + \log^2\psi^{-1}\right)\right), \tag{17}$$

where ψ is the desired accuracy. The evaluation of the gradient is slower using the NUFFT, but it is still faster than (14).

3) Computational Cost Using Differential Contributions for Far Field and Near Field Analysis: The strategy of Differential Contributions (DFC) on the radiated field improves the computational cost of the FFT or NUFFT-based evaluations of the gradient. Although efficient, those methods still compute the contributions from all the elements of the array (N) at all UV points in the spectral domain (M). With the DFC, it is only computed the radiated field (near or far field) of the differential contribution of the kth array element, thus reducing the computational cost in all cases to $\mathcal{O}(M)$. Hence, the new computational cost for evaluating the gradient starting from the tangential field becomes:

$$\mathcal{O}(SM). \tag{18}$$

Finally, the time cost associated to the element analysis (SO_{Elem}) should be included to obtain the time cost for the gradient computation starting from the optimizing variables.

IV. Study of the Improvement in Computing Time

The strategy of differential contributions has been implemented in the generalized Intersection Approach (IA) [14] to accelerate the POS and assess the improvement in the evaluation of the gradient. The generalized IA uses the Levenberg-Marquardt algorithm (LMA) [10] in the backward projector, which requires the computation of the Jacobian matrix, formed with the gradient in (1). The simulations will be carried out in a workstation with an Intel Xeon E5-2630 v4 CPU at 2.2 GHz with 10 cores and 20 threads. The computation of the Jacobian is parallelized computing one derivative (Jacobian column) per thread.

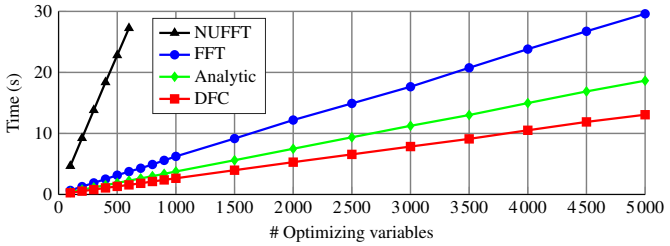

Fig. 2. Measured computing time of the Jacobian matrix evaluation for the far field with the FFT, NUFFT ($\psi = 10^{-2}$), Differential Contributions (DFC) and analytic derivative for different numbers of optimizing variables using a UV grid of 512×512 points and computations parallelized with 20 threads.

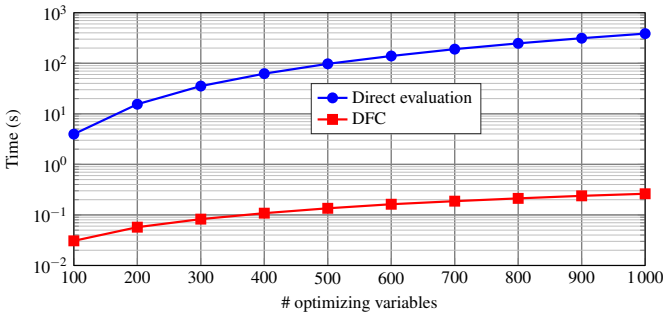

Fig. 3. Measured computing time of the Jacobian matrix evaluation for the near field comparing the direct evaluation and Differential Contributions (DFC) for different numbers of optimizing variables for a Cartesian grid of 6561 points and computations parallelized with 20 threads.

A. Far Field Time Study

For the far field case, the radiation patterns are calculated using the first principle of equivalence, which requires the computation of three spectrum functions for each polarization for POS [14]. Since a periodic grid is a particular case of an aperiodic one, the computing time study will be performed with a periodic grid using the FFT, NUFFT, Differential Contributions (DFC) and the analytical derivative in order to compare the four approaches in the same conditions. In addition, the grid in which the radiation pattern is computed has 512×512 points, which is a typical value for large array synthesis [12]. In this case $\mathcal{O}(O_{\text{Elem}}) = \mathcal{O}(1)$ and $S \ll M$.

Fig. 2 shows the measured computing time when optimizing a different number of array elements, computing the gradient with 20 threads. The precision parameter chosen for the NUFFT is $\psi = 10^{-2}$, which produces fast computations while providing enough accuracy in the computation of the radiation pattern [35]. Using the NUFFT for the computation of the far field results in the slowest of the four techniques for computing the gradient, although it is still much more efficient than the direct evaluation which is not considered in this study. As it can be seen, the DFC is faster than the FFT, NUFFT and even the analytic derivative for the computation of the Jacobian matrix (gradient). In the present case, both the analytic derivative and DFC have a time cost of $\mathcal{O}(SM)$ for the computation of the derivative, but the analytic derivative requires more operations inside the loop sweeping all M points. In addition, the absolute time gaining increases with the number of optimizing variables, which means that time savings will be larger for larger arrays.

The speed up of the DFC technique with regard to the other methods has been calculated from the measured data of Fig. 2 using the following expression:

$$\text{Speed up } (\%) = 100 \cdot \frac{t_{\text{ref}} - t_{\text{DFC}}}{t_{\text{ref}}}, \tag{19}$$

where t_{DFC} is the time employed by the DFC technique and t_{ref} is the time employed by the technique which is compared with the DFC. A mean speed up of 56.9% is obtained for the periodic case (FFT), while a significant speed up for the NUFFT is achieved: 94.2%. Also, the DFC technique is around 29.8% faster than the analytic derivative for the case at hand.

One of the main advantages of the new technique, apart from accelerating the computation of the gradient for array optimization, is the fact that it places the synthesis of aperiodic arrays on the same computing time level as periodic arrays, since for the computation of the gradient there is no need to employ the (NU)FFT. Otherwise, the synthesis of aperiodic arrays could be significantly slower, in light of the computing time shown in Fig. 2 and the study carried out in [35]. In addition, the DFC technique is faster than the analytic derivative thanks to the linearity of the radiated field with regard to the tangential field, which allows to save operations in its computation.

B. Near Field Time Study

The near field is computed following [30]. From the tangential field on the array aperture, expressed in the array coordinate system which is placed at its center, the near field is obtained as far field contributions of all the array elements in a Cartesian grid in planes perpendicular to the pointing direction and expressed in the global coordinate system (see [30] for further reference). For the time study, the near field grid has 6561 points.

Fig. 3 shows the measured computing time for the synthesis of the near field when optimizing different numbers of array elements. As it can be seen, this technique allows to accelerate the computation of the gradient more than two orders of magnitude. Due to the drop in time cost from $\mathcal{O}(SNM)$ to $\mathcal{O}(SM)$ for the computation of the gradient, the DFC technique allows to achieve accelerations of two orders of magnitude when optimizing 100 elements, and up to three orders of magnitude for 1000 elements. In addition, greater accelerations will be achieved when optimizing an even larger number of elements. The mean speed up calculated using (19) is close to 99.8% and the speed up increases with the number of optimizing variables.

C. Errors in the Computation of the Gradient and Scalability

The error in the computation of the Jacobian was recorded, showing that for an implementation with double precision real numbers (8 bytes), the difference between the DFC technique and the analytical computation of a single derivative (i.e. a Jacobian column) is around 10^{-9}. This value is consistent with the expected error in the evaluation of the derivative using

Table I
MEAN SPEED UP OF THE DFC TECHNIQUE WITH REGARD TO OTHER ANALYSIS TECHNIQUES FOR THE COMPUTATION OF THE GRADIENT.

	Speed up (%)			
	Far field			*Near field*
	NUFFT	FFT	Analytical	
1 thread	93.9	57.9	31.0	99.7
20 threads	94.2	56.9	29.8	99.8

finite differences, which for a lateral difference with double precision real numbers (8 bytes) is of the order of $\mathcal{O}(10^{-8})$ [10]. This allows to obtain almost the same results when using the DFC technique in the whole synthesis process as other techniques, but saving considerable amounts of time. The deviations in the obtained phase distributions will be assessed in Section V.

Finally, all previous results were obtained parallelizing the computation of the Jacobian using 20 threads. In order to assess the scalability of the new technique, the study was repeated with a single thread and the measured mean speed up is summarized in Table I. The average speed up is very similar for one and 20 threads, assessing the scalability properties of the proposed technique.

V. SYNTHESIS EXAMPLES

The generalized IA [14] with differential contributions has been employed to perform three array syntheses: two of them in the far field, one for a periodic reflectarray and another for an aperiodic phased-array; and another near field synthesis to improve the quiet zone generated by a reflectarray. The aim is to assess the improvement in computing time and to validate the new technique. In all cases, three iterations of the LMA are performed in the backward projector per iteration of the IA [15].

A. Far Field Synthesis of a Periodic Reflectarray

The first far field synthesis will be that of a periodic reflectarray for DBS application with European coverage [15]. The reflectarray is placed in a geostationary satellite in position 10° E longitude and is comprised of 5180 elements in a rectangular, periodic grid of 74×70 unit cells. The feed is modeled as a $\cos^q \theta$ function with $q = 23$, imposing an illumination taper of -17.9 dB at the reflectarray edges. The feed is placed at (358,0,1070) mm with regard to the reflectarray center. The periodicity of the reflectarray is $14\,\text{mm} \times 14\,\text{mm}$ and the working frequency is 11.85 GHz. The starting point of the synthesis is a pencil beam pattern pointing at $(\theta, \varphi) = (16.26°, 0°)$.

The synthesis was first carried out with the analytical derivative and then using the technique of differential contributions. The obtained phase distributions were compared and their difference is shown in Fig. 4. As it can be seen, the difference in the obtained phases is small, and the larger differences are produced at the edges of the reflectarray. The mean absolute deviation is 1.6° for the results shown in Fig. 4. In addition, the deviation was also computed for the phase distributions

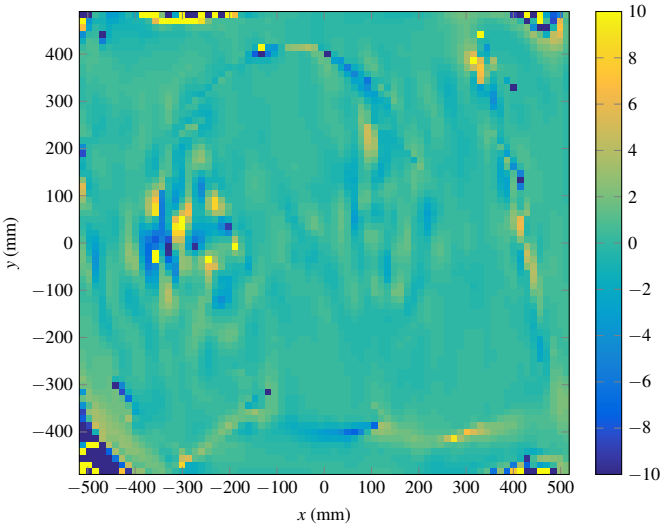

Fig. 4. Phase difference in degrees (°) between the far field syntheses carried out computing the Jacobian matrix (gradient) with analytical derivatives and using finite differences with the technique of differential contributions for the reflectarray with European DBS coverage and X polarization.

Table II
NUMBER OF OPTIMIZING VARIABLES AND LMA ITERATIONS FOR EACH STAGE FOR THE REFLECTARRAY FAR FIELD SYNTHESIS.

Stage	# variables	LMA iterations
1	1042	102
2	2094	138
3	2986	135
4	3910	48
5	4462	24

obtained after the first iteration of the algorithm optimizing all variables at the same time, showing a mean absolute deviation of only 0.0034° ($5.9 \cdot 10^{-5}$ rad). On the other hand, Fig. 5 shows the synthesized copolar patterns for X polarization using both methods. As it can be seen, the differences due to the phase distributions not being the same are negligible. Similar results were obtained for Y polarization regarding the phase distribution and the copolar pattern.

The synthesis took 149 iteration of the generalized IA [14], with three iterations of the LMA [10] per iteration of the IA, thus having a total of 447 iterations where the gradient was computed in multithreaded mode with 20 threads. In addition, the synthesis was carried out in different stages, increasing the number of optimizing variables at each successive stage as shown in Table II. With the technique of differential contributions, a total of 2875 seconds (47.9 minutes) were employed computing the gradient. If the FFT were employed for the computation of the radiation pattern, the computation of the gradient would have taken 6540 seconds (109 minutes), using the data from Fig. 2. This supposes a speed up of roughly 56%, which is in accordance to the data shown in Table I.

Finally, even though it is expected that syntheses that take more iterations to converge will produce larger deviations between the two methods, the results regarding far field

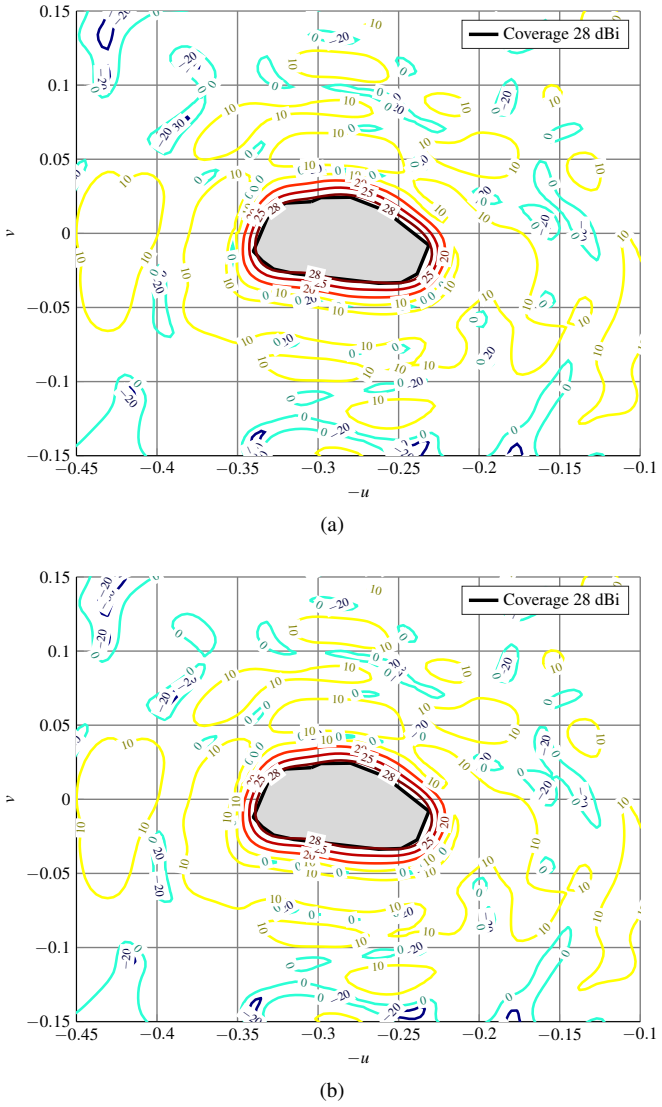

Fig. 5. Copolar pattern for X polarization in gain (dBi) of the synthesized European coverage for DBS application obtained using (a) analytical derivatives and (b) the technique of differential contributions. (u, v) are in the reflectarray coordinate system.

compliance (or near field for those cases), will be good since several solutions are possible for the synthesis problem. The deviation in terms of the obtained phase distribution only means that the optimization algorithm chose a slightly different path across the search space, reaching a different but acceptable solution. In this regard, even though the error in the computation of a single derivative is very small, the fact that the Jacobian requires hundreds or even thousands of derivatives and that very small deviations in the first steps of the algorithm will cause the algorithm to transverse the search space through a different path, causes the phase differences shown in Fig. 4. Hence, in the following sections only the results obtained with the DFC technique will be reported, as well as the time saving derived from using this technique.

B. Far Field Synthesis of an Aperiodic Array

The aperiodic array will be obtained from a periodic array grid adopting the procedure detailed in [36], assuming a raised

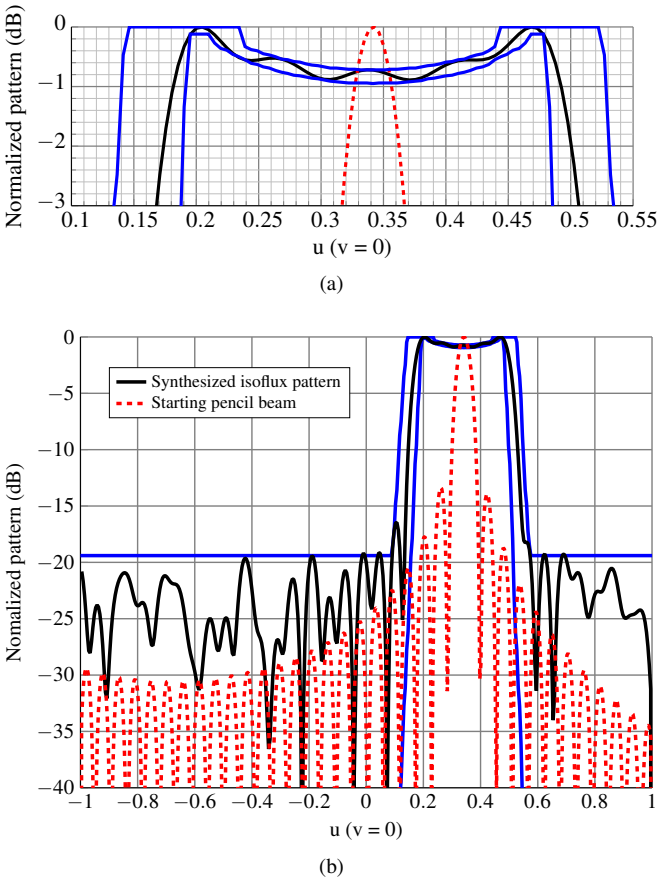

Fig. 6. Result of the optimization of the aperiodic array, showing the starting point for the synthesis (pencil beam; red dotted line) and the final isoflux pattern (black solid line). (a) Zoom of the coverage area for the cut in u. (b) Main cut in u of the radiation pattern.

cosine excitation as starting point and obtaining an aperiodic distribution with uniform excitation. The initial periodic array is rectangular, has a periodicity of $0.4\lambda \times 0.4\lambda$ at 30 GHz and is comprised of 44×44 elements. After applying the procedure in [36] an aperiodic array is obtained. It has the same physical dimensions of the periodic array but it is comprised of 1444 elements, in contrast with the 1936 elements of the periodic array, which supposes a reduction of 25% of the elements. In addition, the local periodicities in the aperiodic array range from 0.41λ to 0.60λ, which avoids the appearance of pseudo-grating lobes.

The goal of the optimization is to obtain an isoflux pattern [37] which will be radiated from a satellite placed in geostationary orbit. The side lobe level is set to -19 dB and the allowed ripple in the coverage area to 0.2 dB, which is a very tight requirement. The starting point is a pencil beam pointing towards the center of the coverage area. After the synthesis, the radiation pattern shown in Fig. 6 was obtained. It is represented along with the pencil beam which was used as starting point. As it can be seen, the obtained isoflux pattern mostly complies with the specification template in both side lobe level and ripple in the coverage area.

In this case, there were 480 gradient evaluations (see Table III), taking 1330 seconds (22.2 minutes) with the technique of differential contributions. If the NUFFT were used, it would

Table III
NUMBER OF OPTIMIZING VARIABLES AND LMA ITERATIONS FOR EACH STAGE FOR THE APERIODIC ARRAY SYNTHESIS WITH ISOFLUX PATTERN.

Stage	# variables	LMA iterations
1	320	33
2	618	105
3	890	63
4	1160	39
5	1290	51
6	1330	111
7	1444	78

have taken 22833 seconds (380.6 minutes, or more than six hours), using the data of Fig. 3 linearly extrapolating the time for the NUFFT with 20 threads, corresponding to a speed up of 94.2%, which is in the range of that reported in Table I.

C. Near Field Synthesis of a Reflectarray

The reflectarray considered for the near field synthesis is square and comprised of 1080 elements in a regular grid of 30×36, with periodicity 6 mm×5 mm. The feed is a horn modeled with a $\cos^q\theta$ function with $q = 8.2$ which generates an illumination taper of -7.4 dB at the reflectarray edges. The working frequency is 20 GHz. As starting point for the optimization, the reflectarray collimates the field in the $\hat{z}$ direction with a radiation angle $\theta_0 = 20°$. The starting phase distribution generates a pencil beam pointing at $(\theta, \varphi) = (20°, 0°)$, while in the near field it collimates the field with the same radiation angle, generating a planar phase front [30]. With this starting point, the quiet zone is strongly limited in amplitude due to the taper imposed by the feed. The goal is to improve the quiet zone size in amplitude while preserving or improving the planar phase front. The imposed specifications are a ripple in amplitude of 1.25 dB, and of 10° in phase.

The synthesis has been carried out in two parallel near field planes placed at 300 mm and 400 mm from the reflectarray center in the global coordinate system [30]. The synthesized near field is shown in Fig. 7, where the main cuts are represented. They correspond to the offset plane for $y = 0$ mm and two different planes perpendicular to the pointing direction $\theta_0 = 20°$ (details of the geometry and antenna optics may be consulted in [30]). As it can be seen, the quiet zone was greatly improved in amplitude, while the phase ripple was also improved.

Finally, the near field synthesis had 3660 evaluations of the gradient in four different stages as shown in Table IV, with a total time of 750 seconds (12.5 minutes) using differential contributions. The same synthesis with the direct evaluation approach would have taken 891342 seconds (10.3 days), thus having a speed up of 99.916%, which is in accordance with the data of Fig. 3, since only sets of more than 500 variables were employed in the different stages of this optimization.

VI. CONCLUSIONS

This paper has presented a technique for the acceleration of gradient-based algorithms implemented with finite differences

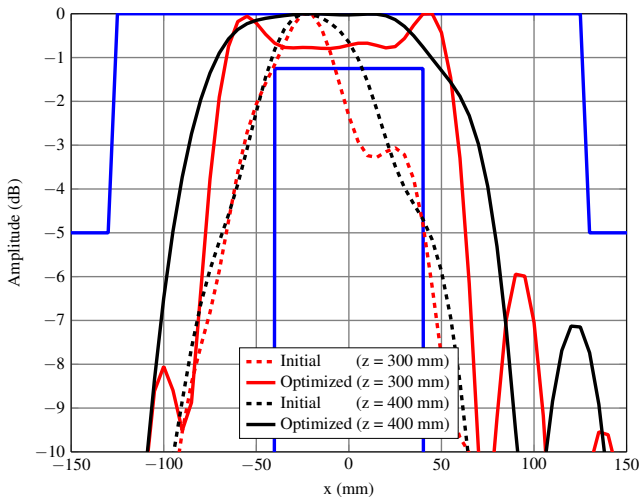

(a)

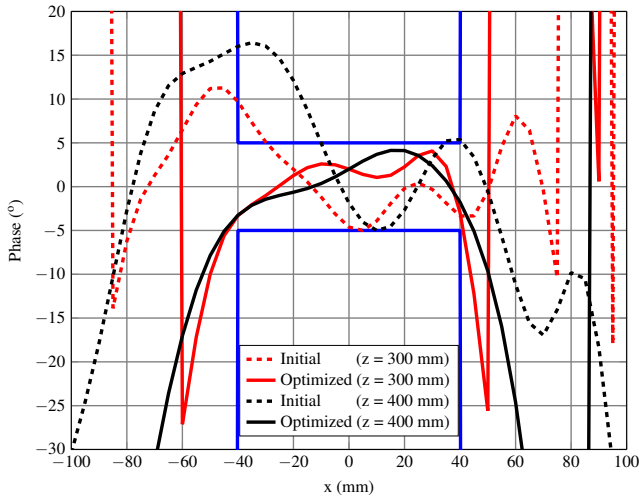

(b)

Fig. 7. Main cuts in the offset plane ($y = 0$ mm) for the initial and synthesized near field at two different planes perpendicular to the collimating direction $\theta_0 = 20°$. (a) Amplitude. (b) Phase.

Table IV
NUMBER OF OPTIMIZING VARIABLES AND LMA ITERATIONS FOR EACH STAGE FOR THE NEAR FIELD SYNTHESIS FOR CATR APPLICATION.

Stage	# variables	LMA iterations
1	580	1260
2	1000	840
3	680	960
4	1000	600

for the optimization of array antennas. It is based on differential contributions (DFC) for the evaluation of the gradient, in which only the contribution of one element is considered for the computation of the radiated field. This way, both far field and near field syntheses are sped up. A time study was carried out comparing the proposed technique with the classic analysis to assess the speed up in the evaluation of the gradient. For the far field analysis with the FFT, employed for periodic arrays, there is a speed up of 57%, while for

the analysis of aperiodic arrays using NUFFT the speed up is around 94%. Furthermore, compared to the use of analytic derivative, the DFC technique is 30% faster due to having less operations for the computation of the gradient. For near field synthesis, the speed up is better than 99.7%. Finally, three different syntheses were carried out to show the performance for each case. First, a large reflectarray comprised of more than 5000 elements was considered for a DBS application with European coverage. The speed up in the gradient evaluation saved an hour (61.1 minutes) in the whole synthesis process (from 109 minutes to 47.9 minutes). Next, an aperiodic array with uniform excitation was optimized to generate an isoflux pattern. This time, the technique of differential contributions saved close to 360 minutes (6 hours) in the evaluation of the gradient in a total of 480 iterations. Finally, the near field synthesis went from taking more than one week evaluating the gradient (10.3 days) to only 12.5 minutes, which supposes a great time saving of more than 99.9%.

REFERENCES

[1] P. M. Woodward, "A method of calculating the field over a plane aperture required to produce a given polar diagram," *J. Inst. Elec. Eng.*, vol. 93, pt. III, no. 10, pp. 1554–1558, 1946.

[2] D. Barbiere, "A method for calculating the current distribution of Tschebyscheff arrays," *Proc. IRE*, vol. 40, no. 1, pp. 78–82, Jan. 1952.

[3] A. Chakraborty, B. N. Das, and G. S. Sanyal, "Beam shaping using nonlinear phase distribution in a uniformly spaced array," *IEEE Trans. Antennas Propag.*, vol. 30, no. 5, pp. 1031–1034, Sep. 1982.

[4] J. M. Johnson and Y. Rahmat-Samii, "Genetic algorithm optimization and its application to antenna design," in *Antennas and Propagation Society International Symposium*, vol. 1, Seattle, Washington, USA, Jun. 20–24, 1994, pp. 326–329.

[5] P. Nayeri, F. Yang, and A. Z. Elsherbeni, "Design of single-feed reflectarray antennas with asymmetric multiple beams using the particle swarm optimization method," *IEEE Trans. Antennas Propag.*, vol. 61, no. 9, pp. 4598–4605, Sep. 2013.

[6] D. W. Boeringer and D. H. Werner, "Particle swarm optimization versus genetic algorithms for phased array synthesis," *IEEE Trans. Antennas Propag.*, vol. 52, no. 3, pp. 771–779, Mar. 2004.

[7] J. Perini and M. Idselis, "Note on antenna pattern synthesis using numerical iterative methods," *IEEE Trans. Antennas Propag.*, vol. 19, no. 2, pp. 284–286, Mar. 1971.

[8] T. S. Fong and R. A. Birgenheier, "Method of conjugate gradients for antenna pattern synthesis," *Radio Sci.*, vol. 6, no. 12, pp. 1123–1130, Dec. 1971.

[9] O. M. Bucci, G. Franceschetti, G. Mazzarella, and G. Panariello, "Intersection approach to array pattern synthesis," *IEE Proc. Microw. Antennas Propag.*, vol. 137, no. 6, pp. 349–357, Dec. 1990.

[10] D. R. Prado, J. Álvarez, M. Arrebola, M. R. Pino, R. G. Ayestarán, and F. Las-Heras, "Efficient, accurate and scalable reflectarray phase-only synthesis based on the Levenberg-Marquardt algorithm," *Appl. Comp. Electro. Society Journal*, vol. 30, no. 12, pp. 1246–1255, Dec. 2015.

[11] Y. Zhang, Z. Zhao, J. Wang, and G. Dan, "Antenna array beam pattern synthesis based on trust region method," in *IEEE 17th International Conference on Computational Science and Engineering*, Chengdu, China, Dec. 19–21, 2014, pp. 859–862.

[12] J. A. Zornoza and J. A. Encinar, "Efficient phase-only synthesis of contoured-beam patterns for very large reflectarrays," *Int. J. RF Microw. Comput. Eng.*, vol. 14, no. 5, pp. 415–423, Sep. 2004.

[13] O. M. Bucci, G. D'Elia, G. Mazzarella, and G. Panariello, "Antenna pattern synthesis: a new general approach," *Proc. IEEE*, vol. 82, no. 3, pp. 358–371, Mar. 1994.

[14] D. R. Prado, M. Arrebola, M. R. Pino, and F. Las-Heras, "Improved reflectarray phase-only synthesis using the generalized intersection approach with dielectric frame and first principle of equivalence," *Int. J. Antennas Propag.*, vol. 2017, pp. 1–11, May 2017.

[15] D. R. Prado, M. Arrebola, M. R. Pino, R. Florencio, R. R. Boix, J. A. Encinar, and F. Las-Heras, "Efficient crosspolar optimization of shaped-beam dual-polarized reflectarrays using full-wave analysis for the antenna element characterization," *IEEE Trans. Antennas Propag.*, vol. 65, no. 2, pp. 623–635, Feb. 2017.

[16] A. Capozzoli, C. Curcio, G. D'Elia, and A. Liseno, "Fast phase-only synthesis of conformal reflectarrays," *IET Microw. Antennas Propag.*, vol. 4, no. 12, pp. 1989–2000, Dec. 2010.

[17] W. M. Dorsey and D. P. Scholnik, "A hybrid global-local optimization approach to phase-only array-pattern synthesis," in *IEEE Radar Conference (RadarCon)*, Arlington, Virginia, USA, May 10–15, 2015, pp. 1417–1422.

[18] J. Álvarez, R. G. Ayestarán, G. León, L. F. Herrán, A. Arboleya, J. A. López-Fernández, and F. Las-Heras, "Near field multifocusing on antenna arrays via non-convex optimisation," *IET Microw. Antennas Propag.*, vol. 8, no. 10, pp. 754–764, Jul. 2014.

[19] T. H. Ismail, D. I. Abu-Al-Nadi, and M. J. Mismar, "Phase-only control for antenna pattern synthesis of linear arrays using the Levenberg-Marquardt algorithm," *Electromagnetics*, vol. 24, no. 7, pp. 555–564, 2004.

[20] M. Zhou, S. B. Sørensen, O. S. Kim, E. Jørgensen, P. Meincke, and O. Breinbjerg, "Direct optimization of printed reflectarrays for contoured beam satellite antenna applications," *IEEE Trans. Antennas Propag.*, vol. 61, no. 4, pp. 1995–2004, Apr. 2013.

[21] P. Robustillo, J. Zapata, J. A. Encinar, and J. Rubio, "ANN characterization of multi-layer reflectarray elements for contoured-beam space antennas in the Ku-band," *IEEE Trans. Antennas Propag.*, vol. 60, no. 7, pp. 3205–3214, Jul. 2012.

[22] D. R. Prado, J. A. López-Fernández, G. Barquero, M. Arrebola, and F. Las-Heras, "Fast and accurate modeling of dual-polarized reflectarray unit cells using support vector machines," *IEEE Trans. Antennas Propag.*, vol. 66, no. 3, pp. 1258–1270, Mar. 2018.

[23] H. Akel and J. P. Webb, "Design sensitivities for scattering-matrix calculation with tetrahedral edge elements," *IEEE Trans. Magn.*, vol. 36, no. 4, pp. 1043–1046, Jul. 2000.

[24] S. Koziel, F. Mosler, S. Reitzinger, and P. Thoma, "Robust microwave design optimization using adjoint sensitivity and trust regions," *Int. J. RF Microw. Comput. Eng.*, vol. 22, no. 1, pp. 10–19, Jan. 2012.

[25] M. Ghassemi, M. Bakr, and N. Sangary, "Antenna design exploiting adjoint sensitivity-based geometry evolution," *IET Microw. Antennas Propag.*, vol. 7, no. 4, pp. 268–276, Mar. 2013.

[26] S. Koziel and A. Bekasiewicz, "Fast EM-driven size reduction of antenna structures by means of adjoint sensitivities and trust regions," *IEEE Antennas Wireless Propag. Lett.*, vol. 14, pp. 1681–1684, 2015.

[27] M. Bakr, A. Elsherbeni, and V. Demir, *Adjoint sensitivity analysis of high frequency structures with MATLAB®*. Edison, NJ, USA: SciTech Publishing, 2017.

[28] J. Huang and J. A. Encinar, *Reflectarray Antennas*. Hoboken, NJ, USA: John Wiley & Sons, 2008.

[29] A. Capozzoli, C. Curcio, A. Liseno, and G. Toso, "Fast, phase-only synthesis of aperiodic reflectarrays using NUFFTs and CUDA," *Progr. Electromagn. Res.*, vol. 156, pp. 83–103, 2016.

[30] D. R. Prado, A. F. Vaquero, M. Arrebola, M. R. Pino, and F. Las-Heras, "General near field synthesis of reflectarray antennas for their use as probes in CATR," *Progr. Electromagn. Res.*, vol. 160, pp. 9–17, Oct. 2017.

[31] O. M. Bucci, G. Mazzarella, and G. Panariello, "Reconfigurable arrays by phase-only control," *IEEE Trans. Antennas Propag.*, vol. 39, no. 7, pp. 919–925, Jul. 1991.

[32] D. M. Pozar and T. A. Metzler, "Analysis of a reflectarray antenna using microstrip patches of variable size," *Electron. Lett.*, vol. 29, no. 8, pp. 657–658, Apr. 1993.

[33] C. Wan and J. A. Encinar, "Efficient computation of generalized scattering matrix for analyzing multilayered periodic structures," *IEEE Trans. Antennas Propag.*, vol. 43, no. 11, pp. 1233–1242, Nov. 1995.

[34] J. Rubio, M. A. Gonzalez, and J. Zapata, "Generalized-scattering-matrix analysis of a class of finite arrays of coupled antennas by using 3-D FEM and spherical mode expansion," *IEEE Trans. Antennas Propag.*, vol. 53, no. 3, pp. 1133–1144, Mar. 2005.

[35] D. R. Prado, M. Arrebola, M. R. Pino, and F. Las-Heras, "An efficient calculation of the far field radiated by non-uniformly sampled planar fields complying Nyquist theorem," *IEEE Trans. Antennas Propag.*, vol. 63, no. 2, pp. 862–865, Feb. 2015.

[36] S. Suárez, G. León, M. Arrebola, L. F. Herrán, and F. Las-Heras, "Experimental validation of linear aperiodic array for grating lobe suppression," *Progr. Electromagn. Res. C*, vol. 26, pp. 193–203, 2012.

[37] D. R. Prado, A. Campa, M. Arrebola, M. R. Pino, J. A. Encinar, and F. Las-Heras, "Design, manufacture and measurement of a low-cost reflectarray for global Earth coverage," *IEEE Antennas Wireless Propag. Lett.*, vol. 15, pp. 1418–1421, 2016.

Daniel R. Prado was born in Sama de Langreo, Asturias, Spain, in 1986. He received the B.Sc., M.Sc., and Ph.D. degrees in telecommunication engineering from the University of Oviedo, Gijón, Spain in 2011, 2012, and 2016 respectively.

From September 2010 to March 2011 he was with The Institute of Electronics, Communications and Information Technology (ECIT), Queen's University Belfast, Belfast, U.K., working on the design of leaky-wave antennas as part of his B.Sc. research project. From 2011 to 2017, he was a Research Assistant with the Signal Theory and Communications Area, University of Oviedo, working on the development of efficient techniques for the analysis and synthesis of reflectarray antennas. From August to November 2014 he was with the School of Electrical Engineering, KTH Royal Institute of Technology, Stockholm, Sweden, as a Visiting Scholar, where he worked in transformation optics applied to dielectric lenses. Since January 2018, he has been with the Institute of Sensors, Signals and Systems, Heriot-Watt University, Edinburgh, U.K. His current research activities include analysis of non-uniform arrays, and the development of efficient techniques for the analysis and optimization of near and far fields of reflectarray antennas.

Dr. Prado was the recipient of a predoctoral scholarship financed by Gobierno del Principado de Asturias, and a postdoctoral fellowship partially financed by the European Union.

Álvaro F. Vaquero was born in Salinas, Asturias, Spain in 1990. He received the B.Sc. and M.Sc. degrees in telecommunication engineering from the University of Oviedo, Gijón, Spain, in 2015 and 2017, respectively, where he is currently pursuing the Ph.D. degree.

Since September 2016, he has been working as a Research Assistant with the Signal Theory and Communications Area, University of Oviedo. From September to November 2017, he was with the Instituto de Telecomunicações, Instituto Superior Técnico of Lisbon, Portugal, where he worked on broadband planar lenses for skin cancer imaging. His research interests include the development of efficient techniques for the analysis and synthesis of reflectarrays and planar lenses as well as the design of 3D printed lenses for imaging applications.

Manuel Arrebola (S'99–M'07–SM'17) was born in Lucena (Córdoba), Spain. He received the Ingeniero de Telecomunicación degree from the Universidad de Málaga (UMA), Málaga, Spain, in 2002, and the Ph.D. degree from the Universidad Politécnica de Madrid (UPM), Madrid, Spain, in 2008.

From 2003 to 2007, he was with the Electromagnetism and Circuit Theory Department at UPM as a Research Assistant. From August to December 2005, he was with the Microwave Techniques Department at the Universität Ulm, Ulm, Germany, as a Visiting Scholar. In December 2007, he joined the Electrical Engineering Department at the Universidad de Oviedo, Gijón, Spain, where he is an Associate Professor. In 2009, he enjoyed a two-month stay at the European Space Research and Technology Centre, European Space Agency (ESTEC-ESA), Noordwijk, The Netherlands. His current research interests include analysis and design techniques of contoured-beam and reconfigurable printed reflectarrays both in single and dual-reflector configurations and planar antennas.

Dr. Arrebola was co-recipient of the 2007 S.A. Schelkunoff Transactions Prize Paper Award, given by the IEEE Antennas and Propagation Society.

Marcos R. Pino was born in Vigo, Spain, in 1972. He received the M.Sc. and Ph.D. degrees in telecommunication engineering from the University of Vigo, Spain, in 1997 and 2000, respectively.

During 1998, he was a Visiting Scholar at the ElectroScience Laboratory, The Ohio-State University, Columbus (OH). From 2000 to 2001 he was Assistant Professor at the University of Vigo. Since 2001, he has been with the Electrical Eng. Department, University of Oviedo, Spain, where he currently is Associate Professor teaching courses on communication systems and antenna design. His current research areas are antenna design, measurement techniques and efficient computational techniques applied to EM problems such as evaluation of radar cross section or scattering from rough surfaces.

Fernando Las-Heras (M'86–SM'08) received the M.Sc. and Ph.D. degrees in telecommunication engineering from the Technical University of Madrid, Madrid, Spain (UPM), in 1987 and 1990, respectively.

From 1988 to 1990, he was a National Graduate Research Fellow at UPM, Madrid. From 1991 to 2000 he was an Associate Professor with the Department of Signal, Systems, and Radiocommunications, UPM. He was a Visiting Lecturer at the National University of Engineering, Lima, Peru, in 1996; Syracuse University, Syracuse, NY, USA, in 2000; and a short-term Visiting Lecturer at ESIGELEC, Sain-Étienne-du-Rouvray, France from 2005 to 2011. Since 2001, he heads the research group Signal Theory and Communications TSC-UNIOVI, Department of Electrical Engineering, University of Oviedo. Since December 2003, he has been a Full-Professor with the University of Oviedo, Gijón, Spain, where he was the Vice-Dean of Telecommunication Engineering at the Technical School of Engineering from 2004 to 2008. From 2005 to 2015, he held the Telefónica Chair on RF Technologies, ICTs applied to Environment and ICTs and Smartcities with the University of Oviedo. He was a member of the board of directors of the IEEE Spain Section from 2012 to 2015; the board the IEEE Microwaves & Antennas Propagation Chapter (AP03/MTT17) from 2016 to 2017; the Science, Technology and Innovation Council of Asturias since 2010; and the President of the professional association of Telecommunication Engineers, Asturias. He has led and participated in a great number of research projects and has authored over 190 technical journal papers, mainly in the areas of antennas, propagation, metamaterials and inverse problems with application to antenna measurement (NF-FF, diagnostics, and holography), electromagnetic imaging (security and NDT), and localization, developing computational electromagnetics algorithms and technology on microwaves, millimeter wave, and THz frequency bands.